



Statistical analysis of interplanetary coronal mass ejections and their geoeffectiveness during the solar cycles 23 and 24

P. Alexakis¹ · H. Mavromichalaki¹

Received: 21 May 2019 / Accepted: 24 October 2019
© Springer Nature B.V. 2019

Abstract Interplanetary coronal mass ejections (ICMEs) are believed to be the most common and important drivers of the strongest geomagnetic storms. In this work, the geoeffective characteristics of the ICMEs occurred during the last solar cycles 23 and 24 (years 1996–2017) have been studied in detail. The maximum velocity V_{\max} , either of the ICME's Sheath region or of the ICME itself, the mean velocity of the ICME, the minimum value of the southward component of the Interplanetary magnetic field B_s and the y -component of the solar wind convective electric field $E = -V \times B$ observed at L1 point during the pass of the ICME, were used. It was found that, in accordance to past similar studies, the most dominant characteristic of ICMEs in the generation of geomagnetic storms is the B_s component along with the E_y parameter, while the maximum velocity seems to be of less importance. Nevertheless the maximum speed is an good forecasting factor due to the fact that it is much easier to estimate the velocity of an ICME-structure many hours before it arrives at Earth compared with the observations of B_s and E_y that can only be done, for the time being, at the L1 point. That means we can use the velocity of ICME-structure to forecast the possible generation and magnitude of the geomagnetic storms. From a comparison of the ICME-generated geomagnetic storms with the total number of geomagnetic storms generated during the last two solar cycles, it seems that approximately half of the ICMEs (49% for Dst index and 53% for Kp index) produced geomagnetic storms during the solar cycles 23 and 24. Moreover the velocities of ICMEs are more in accordance with the rising and

maximum phases of solar cycles 23 and 24 than the geomagnetic activity (storms) are, as well as during the first stages of the declining phases of these cycles, especially during solar cycle 23.

Keywords Interplanetary coronal mass ejections · Geomagnetic storm · Solar cycle · Statistical analysis

1 Introduction

The solar wind structures that are transported throughout the interplanetary space can cause disturbances on the Earth's magnetic field. These are called geomagnetic disturbances and the most severe of them are called geomagnetic storms (GSs) (Zhang and Burlaga 1988; Gosling et al. 1991; Gonzalez et al. 1994; Tsurutani and Gonzalez 1997; Feynman and Gabriel 2000; Richardson et al. 2001; Daglis et al. 2003; Zhang et al. 2007). These storms, depending on their intensity, can cause many physical, technological and health effects on space and ground-based systems and human activity (Thomson et al. 2005; Rama et al. 2009; Welling 2010; Lakhina and Tsurutani 2016; Galata et al. 2017). The main mechanism behind geomagnetic storms is the magnetic reconnection between the south component of the interplanetary magnetic field (IMF) and the Earth's magnetic field (e.g. Dungey 1961; Gonzalez et al. 1994, 1999; Echer et al. 2008, 2017 and references therein). During this process, energy and magnetic flux are transferred from the solar wind and its structures inside the Earth's magnetosphere. It is believed that the most intense storms are mainly caused by the interplanetary manifestation of coronal mass ejections, i.e. the Interplanetary Coronal Mass Ejections (ICMEs) (Gosling et al. 1991; Zhang et al. 2007; Mustajab and Badruddin 2011; Wu et al. 2013; Paouris and

✉ H. Mavromichalaki
emavromi@phys.uoa.gr

P. Alexakis
panosalex@phys.uoa.gr

¹ Faculty of Physics, National and Kapodistrian University of Athens, 15784 Athens, Greece

Mavromichalaki 2017a, 2017b). These structures can carry intense south component of the IMF, leading to intense geomagnetic disturbances. They can be measured globally by ground magnetometers located all over the Earth's surface with the use of the so called geomagnetic indices (Mayaud 1980). Each geomagnetic index describes usually different physical phenomena and is measured at different latitudes, for example the AL and AE indices measure the global auroral electrojet activity at polar regions, the Kp index measure the disturbances of the field-aligned currents at mid-latitudes and the Dst index measure the intensity of the ring current system near the equator (Borovsky and Shprits 2017). They are calculated by estimating the variations in the magnitude of the horizontal component of the local geomagnetic field, which are directly linked to the variations in the geomagnetic current system (Mayaud 1980; Menvielle and Berthelier 1991). Thus, the geomagnetic disturbances that are produced by the solar wind and its structures (e.g. ICMEs), can be measured, to their intensity, by the geomagnetic indices.

One of the major targets of space weather forecasting is the accurate prediction of the arrival time of the disturbances of solar wind. To succeed in this achievement, the scientific community needs to understand the behavior of the solar wind, especially during disturbed times, that may generate strong geomagnetic activity. Our study aims to this direction by doing a statistical analysis of the ICMEs and their geoeffectiveness to improve their forecasting, by correlating their most geoeffective characteristics with their impact on the magnetosphere.

2 Data selection

In order to examine and analyse the geoeffectiveness of the ICMEs described in the catalogue of Richardson and Cane (www.srl.caltech.edu/ACE/ASC/DATA/level3/icmetable2.htm) occurred during the last two solar cycles 23 and 24 (1996–2017), hourly averaged plasma data for solar wind-ICMEs and geomagnetic indices from the GSFC/SPDF OMNIWeb (omniweb.gsfc.nasa.gov) and World Data Center for Geomagnetism (wdc.kugi.kyoto-u.ac.jp/) databases, were used. In this work data of the geomagnetic indices Kp and Dst were used in order to analyse the geoeffectiveness of the ICMEs. Also, data of the 13-month smoothed sunspot number (SSN) was obtained from the World Data Center-SILSO database (sidc.be/silso/home).

A statistical analysis of the ICMEs velocities and their association with geomagnetic storms (GSs) and also a study of the geoeffectiveness of some characteristic plasma parameters of these ICMEs was performed. The classification of the GSs according to the mentioned geomagnetic indices Kp and Dst, is shown in Table 1. That is, according to Kp index

Table 1 Geomagnetic Storms classification. The Kp-classification is based on the NOAA “G” Scale (<https://www.swpc.noaa.gov/noaa-scales-explanation>) and the Dst-classification is according to Loewe and Pröls (1997) classification

Storms scale (Dst)	Dst values	Storms scale (Kp)	Kp values
Moderate	$-100 < \text{Dst} \leq -50$ nT	G1	Kp = 5
Strong	$-200 < \text{Dst} \leq -100$ nT	G2	Kp = 6
Severe	$-350 < \text{Dst} \leq -200$ nT	G3	Kp = 7
Great	$\text{Dst} \leq -350$ nT	G4	Kp = 8
		G5	Kp = 9

the NOAA “G” scale (<https://www.swpc.noaa.gov/noaa-scales-explanation>) and according to Dst the Loewe and Pröls (1997) scale for GSs. A number of 502 ICMEs during the solar cycles 23 and 24 obtained from the catalogue of Richardson and Cane were examined in this work, either they were associated with a leading shock region or not, excluding 7 of them due to the lack of data. Moreover, both the maximum velocity of the structure heading to Earth (either of ICME/sheath or the shock) and the mean velocity of the ICME, the south component B_s of the magnetic field of the ICME and the dawn-to-dusk convective electric field E_y (in GSE coordinates) which is believed to play an important role in the magnetic reconnection mechanism at the dayside of the Earth's magnetosphere, thus an important role at energy injection in the magnetosphere were analyzed (Dungey 1961; Owens et al. 2005; Ji et al. 2010). This study focuses on connecting these plasma parameters of the ICMEs and their possible shock with the geomagnetic activity and the thresholds of each GS category based on Kp and Dst indices, that ICMEs may produce. A correlation study of the geoeffectiveness of ICMEs with the total number of geomagnetic storms during the last solar cycles 23 and 24 was also carried out.

A typical sample of the ICMEs catalogue of Richardson and Cane (2019) is given in Table 2. In this Table the first column of the catalogue shows the time of the disturbance, measured by ground magnetometers, or the possible shock measured by ACE, WIND or SOHO CELIAS/MTOF/PM spacecrafts. In the second and third columns the start and the end times of the ICME are presented respectively. In fourth and fifth columns there are the start and end times of the associated interval of abnormal solar wind composition/charge states in hours relative to the start and end times of the ICME (data available from 1998 and thereafter). The sixth and seventh columns give the start and end times of the Magnetic Clouds (MCs), in hours relative to the ICME leading or trailing edges. In the eighth and ninth columns we have evidence of BiDirectional suprathermal Electron strahls (BDE) and BiDirectional energetic Ion Flows (BIF). The tenth column gives the “quality” of the boundary times

Table 2 A typical sample of the ICMEs catalogue of Richardson and Cane (2019) from 1996 up to date (www.srl.caltech.edu/ACE/ASC/DATA/level3/icmetable2.htm)

Disturbance Y/M/D (UT) (a)	ICME Plasma/Field Start, End Y/M/D (UT) (b)		Comp. Start, End (Hrs wrt. Plasma/ Field) (c)		MC Start, End (Hrs wrt. Plasma/ Field) (d)		BDE? (e)	BIF? (f)	Qual. (g)	dV (km/s) (h)	V_ICME (km/s) (i)	V_max (km/s) (j)	B (nT) (k)	MC? (l)	Dst (nT) (m)	V_transit (km/s) (n)	LASCO CME Y/M/D (UT) (o)
1996/05/27 1500	1996/05/27 1500	1996/05/29 0300	0	+4	N	...	2	0	370	400	9	2	-33	...	
1996/07/01 1320	1996/07/01 1800	1996/07/02 1100	0	0	N	...	3	40	360	370	11	2	-20	...	
1996/08/07 0600	1996/08/07 1200	1996/08/08 1000	0	0	N	...	2	10	350	380	7	2	-23	...	
1996/12/23 1600	1996/12/23 1700	1996/12/25 1100	+10	0	N	...	2	20	360	420	10	2	-18	435	1996/12/19 1630 H
Disturbance Y/M/D (UT) (a)	ICME Plasma/Field Start, End Y/M/D (UT) (b)		Comp. Start, End (Hrs wrt. Plasma/ Field) (c)		MC Start, End (Hrs wrt. Plasma/ Field) (d)		BDE? (e)	BIF? (f)	Qual. (g)	dV (km/s) (h)	V_ICME (km/s) (i)	V_max (km/s) (j)	B (nT) (k)	MC? (l)	Dst (nT) (m)	V_transit (km/s) (n)	LASCO CME Y/M/D (UT) (o)
1997/01/10 0104	1997/01/10 0400	1997/01/11 0200	0	0	Y	...	1	100 S	450	460	14	2	-78	507	1997/01/06 1510 H
1997/02/09 1321	1997/02/10 0200	1997/02/10 1900	0	0	Y	...	2	90 S	450	600	8	2	-68	683	1997/02/07 0030 H
1997/04/10 1745	1997/04/11 0600	1997/04/11 1900	0	0	Y	...	1	150	460	470	20	2	-82	552	1997/04/07 1427 H
1997/04/21 0600	1997/04/21 1000	1997/04/23 0400	+4	+2	Y	...	2	40	360	420	12	2	-107	...	
1997/05/15 0159	1997/05/15 0900	1997/05/16 0000	0	0	N	Y	1	150 S	450	480	21	2	-115	616	1997/05/12 0530 H
1997/05/26 0957	1997/05/26 1600	1997/05/27 1000	0	+9	Y	...	2	70 S	340	350	10	2H	-74	381	1997/05/21 2100
1997/06/08 1636	1997/06/08 1800	1997/06/10 0000	+8	0	Y	...	3	30	380	400	12	2	-84	...	
1997/06/19 0032	1997/06/19 0700	1997/06/20 2300	-2	-31	Y	Y	2	60	360	390	8	2	-36	...	
1997/07/15 0311	1997/07/15 0800	1997/07/16 1100	0	-11	Y	Y	2	80	350	360	10	2	-45	...	
1997/08/03 1042	1997/08/03 1300	1997/08/04 0300	0	0	Y	...	1	80	400	480	16	2	-48	410	1997/07/30 0445 H

of the ICME. At the eleventh column the acceleration of the upstream disturbance (shock/wave) estimated from 1-hour averaged solar wind data (with shock indication from ACE) is given. The twelfth to fourteenth columns give the mean ICME velocity, the maximum solar wind velocity during the passage of the ICME and the mean magnetic field strength of the ICME respectively. In the fifteenth column we see if the ICME had or not any MC evidence. In the sixteenth column there is the minimum Dst value from the ICME passage. In the seventeenth and eighteenth columns the mean 1 AU transit velocity of the disturbance based on the possible CME association of the ICME from SOHO/LASCO or STEREO spacecrafts are given.

3 Results

3.1 Geomagnetic storms and ICMEs

Our results revealed that during the last two solar cycles (1996–2017) half of the ICMEs were associated with geomagnetic storms (GSs) and only ~20% of the ICMEs with strong GSs ($Dst < -100$ nT/ $Kp \geq 7$) (see Sects. 3.2 and 3.3), even though they are considered as important drivers of the intense GSs. The 13-month smoothed solar sunspot number, obtained by the World Data Center-SILSO (upper panel), the annual number of GSs based on the Kp and on Dst indices (middle panels) and (the yearly number of all ICMEs, the annual number of ICMEs associated with GSs based on Kp (green color) and based on Dst (red color) as well (last panel) during the two solar cycles 23 and 24, are

shown in Fig. 1. We can see that for the cycle 23 (1996–2008) a very good relation of SSN and the number of ICMEs is presented, where the number of ICMEs follows the solar cycle with a maximum at the year 2000, near the solar maximum of the sunspot number at the year 2001 and a corresponding minimum at the year 2008. The number of GSs does not follow exactly the same feature, as they present a maximum at the year 2003 and a minimum at 2009, that means a slight forwarding shift for about ~1 year. For solar cycle 24 the number of ICMEs presents a maximum two years before the solar maximum at the year 2014 and the number of GSs has their maximum again one year after the solar maximum.

It is clear that ICMEs do not follow exactly the motivation of strong geomagnetic activity (i.e. the geomagnetic storms), especially during the declining phase of the solar cycle, where the number of geomagnetic storms decreases, although there is an increase in the number of the ICMEs produced GSs (during both cycles, mainly in the years 2005 and 2015). However, they seem to follow really well the rising phase of solar cycle, indicating that geomagnetic activity is more affected by the ICMEs during the rising phase rather than the declining phase of solar cycles (Gonzalez et al. 1999, 2011; Gopalswamy et al. 2014; Gerontidou et al. 2018). For example, at the year 2003 (declining phase) a dramatic increase of geomagnetic activity but not in the number of ICMEs (only 22 where 14 of them were generated by a GS) was observed.

The geomagnetic storm-related ICMEs (red and green color at Fig. 1d) also show the same behavior, especially

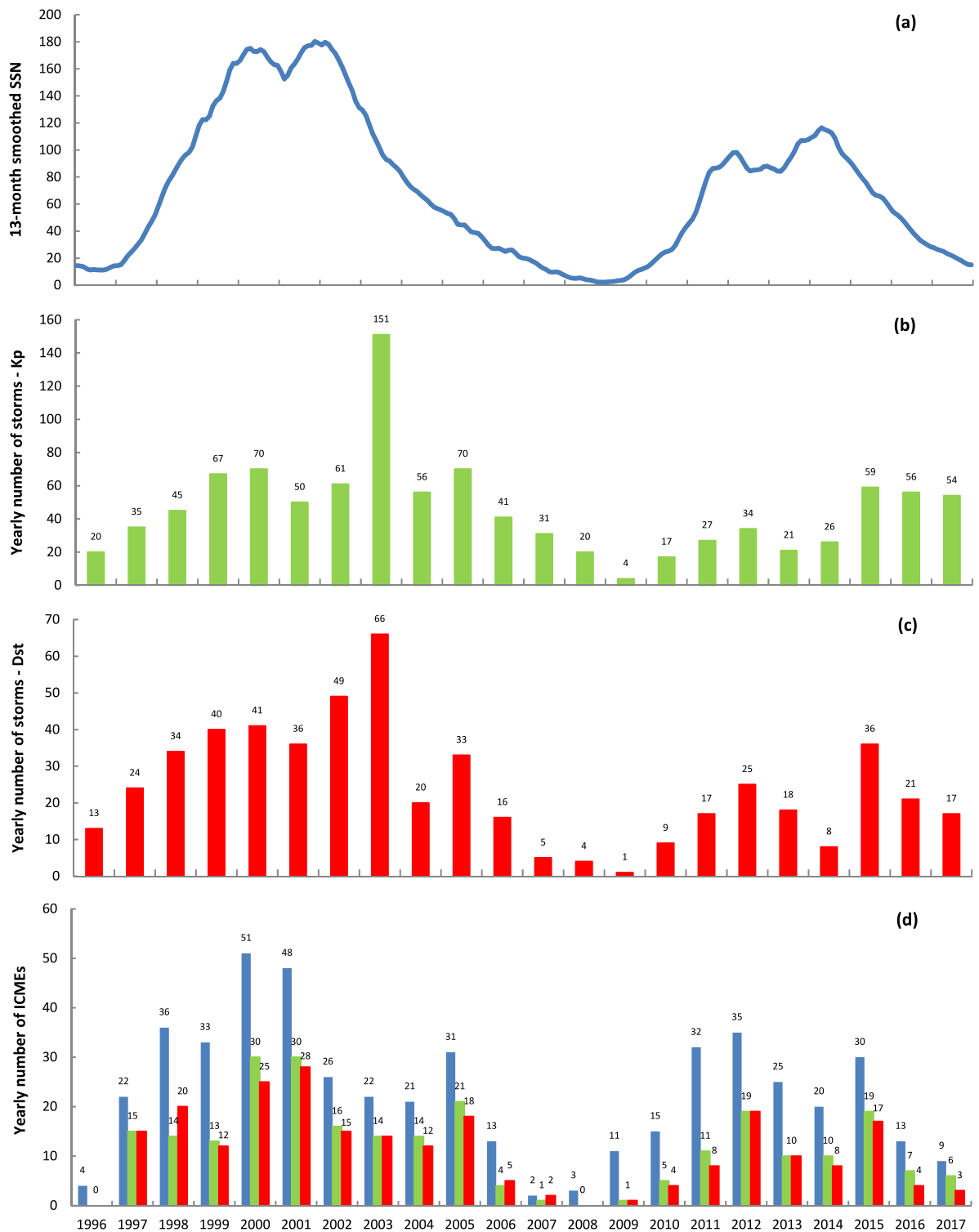


Fig. 1 (a) The 13-month smoothed sunspot number (SSN), (b) the annual number of geomagnetic storms (GSs) according to Kp index, (c) the annual number of GSs according to Dst index and (d) the annual number of ICMEs during the solar cycles 23 and 24 (1996–2017) are

presented. In this last panel the total number the ICMEs (blue color), the ICMEs generated a GS according to Kp index (green color) and the ICMEs generated a GS according to Dst index (red color) are presented. Above the bars the corresponding values are indicated

during the declining phases of the cycles, where the ratio of ICMEs/Geoeffective-ICMEs drops (as Geoeffective-

ICMEs are considered the ICMEs generated a GS). This probably means that during the declining phases of these

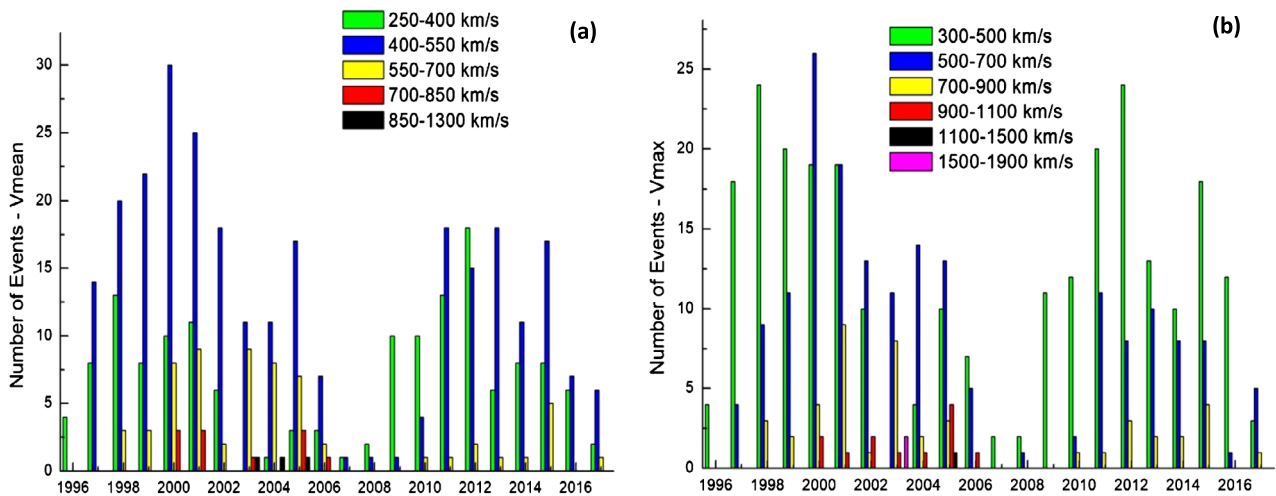


Fig. 2 Yearly distribution of the V_{mean} (left panel) and of the V_{max} (right panel) velocity of ICMEs for each range (in colors) during the years 1996–2017

two solar cycles there is an increase, in number, of other solar sources that generate this increased geomagnetic activity, such as high speed solar wind streams from coronal holes (Gonzalez et al. 1999, 2011; Gerontidou et al. 2018). Nevertheless, the general behavior remains the same, at solar cycle 23 the ICMEs (and the GSs) are larger in numbers and geoeffectiveness than in the corresponding ones of the cycle 24. This result is consistent with the observed results that the even solar cycles (such as the cycle 24) are less active than the odd ones (such the cycle 23) in general activity (Mavromichalaki and Vassilaki 1998; Gerontidou et al. 2018), and also that the plasma parameters of ICMEs at solar cycle 23 are higher than in solar cycle 24 (Chi et al. 2016).

We didn't notice any dramatic difference between the Kp-associated and Dst-associated geomagnetic storms (Fig. 1d) due to the ICMEs. However, during the data analysis we noticed some differences between these two “kinds” of GSs. For example we noticed some ICMEs with sufficient B_s and E_y that generated high Dst values but low Kp values (e.g. 29/8/2004, 14/1/2007 etc.), or with low B_s , E_y and Dst reduction and average speed they gave high Kp (4/6/2011), or ICMEs with almost identical velocities, B_s and E_y and same Kp generated different Dst reductions (e.g. 10/4/2015 and 6/5/2015). We can also see that the Dst-GSs seem to follow slightly better the annual numbers of the ICMEs which means that Kp index is more easily affected by other drivers. All these differences can be explained by the fact that both the Kp and Dst indices are affected by different physical current systems, i.e. different magnetospheric currents and thus a little different number of these two categories of GSs are observed. It is known that the Dst index is affected by the ring current system and the Kp is affected by the field aligned Birkeland currents and

the magnetopause-magnetotail current (Ganushkina et al. 2018).

The yearly distribution of ICMEs velocities (mean and max, according to Richardson and Cane's ICMES catalogue) over the last two solar cycles (1996–2017) is illustrated in Fig. 2. It is well known that ICMEs are the main drivers of intense GSs during the rising phases and maximums of solar cycles (e.g. Gonzalez et al. 2011), and our results are in accordance with these past results (Fig. 1 and 2). During the rising phase of solar cycles 23 and 24 we have an increase in number of medium and high velocities (blue and yellow lines in Fig. 2) of the ICMEs compared to the lower velocities (green color), which is much more clear in cycle 23 than 24. During the declining phases of both cycles we have a clear decrease of slower ICMEs and an increase in faster ICMEs (yellow and red color) and also a small occurrence rate of extremely high velocity events (black and pink) in cycle 23. More specifically, in cycle 23 we had 3 extreme velocity events (black and pink) and we also see fast events in the declining phase of cycle 24 (comparing with the low-velocity events of this cycle). These results suggest that during the rising phases we have an increase of ICME events, in almost all velocity ranges, at the solar maximum we have a decrease in low-velocity and an increase in mid and high-velocity ICMEs (where their geoeffectiveness will normally increase) and at the declining phase we have a persistence in mid and high-velocity ICMEs and a small occurrence of very high-velocity ICMEs (comparing to the general velocities background for each cycle), especially for cycle 23.

Despite the moderate correlations between the mean and maximum velocities of the ICMEs with their geoeffectiveness (see Sects. 3.2 and 3.3), an increase in these velocities seems to enhance their geoeffectiveness. This is confirmed by Fig. 1 (b and c) where we see an increase in the number of GSs during the intervals where there was an increase

in ICMEs velocities (maximum and declining phases of the solar cycles).

3.2 ICMEs and Kp index

The number of ICME events that led or not, to geomagnetic storms (GS) during their passage from the magnetosphere, according to the Kp index (NOAA “G” scale) are shown in Fig. 3. We can see that ICMEs’ or sheaths’ geoeffectiveness (Tsurutani et al. 1988; Huttunen et al. 2005;

Owens et al. 2005; Zhang et al. 2007) can contribute to almost all possible levels (except level zero $K_p = 0$). The mean value of Kp is ~ 4.7 , corresponding to $K_p = 5^-$ according to NOAA “G” scale.

Note that we have used the integer and not the decimal values of Kp index. The percentages of ICME events that triggered the creation of a GS were found to be $\sim 53\%$ (263 out of 495 ICMEs), where 47% (232 out of 495 ICMEs) didn’t lead to a GS. We also see that $\sim 20\%$ (98 events) of the events generated a G1 storm, $\sim 16\%$ (81 events) generated a G2 storm, 10% (49 events) a G3, 4% (21 events) a G4 storm and 3% (14 events) a G5 storm. In Fig. 4 we can see the correlation of maximum Kp index occurred during the passage of the ICME (and the possible sheath/shock regions), with (a) the max and (b) the mean ICME velocities during the event passing from the magnetosphere. It’s clear that there is an increase in the level of storms with the increase of velocities, but correlations are in moderate levels ($cc = 0.56$ for both).

The minimum value of the southward component B_s of the IMF of the ICME (left panel), and the maximum value of the dawn-to-dusk E_y convective field at L1 point versus the Kp values of each event are given in Fig. 5. It seems that the Kp index has a better correlation with these two plasma parameters ($cc = -0.74$ with B_s and 0.72 with E_y) than the maximum and mean velocities of the ICMEs. This means that these can be more suitable forecasting parameters than the ICME maximum and mean values of velocity (Richard-

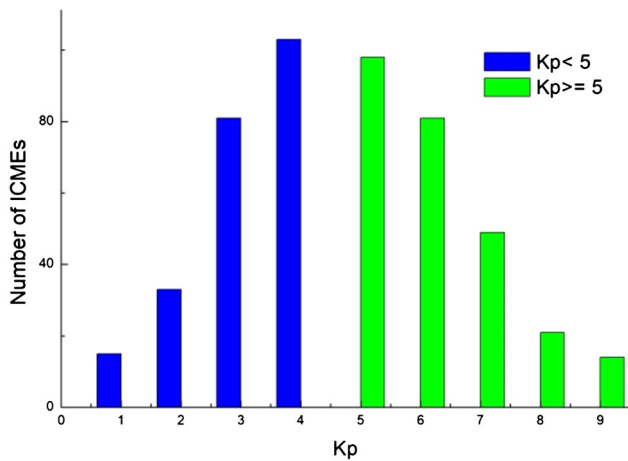


Fig. 3 The number of ICMEs not associated with geomagnetic storms ($K_p \leq 4$, blue color) and the number of ICMEs associated with geomagnetic storms ($K_p > 4$, green color) versus the Kp values

Fig. 4 Correlation diagram of the ICME V_{max} (left panel) and of the ICME V_{mean} (right panel) during their passage from the magnetosphere versus of the Kp index during the years 1996–2017

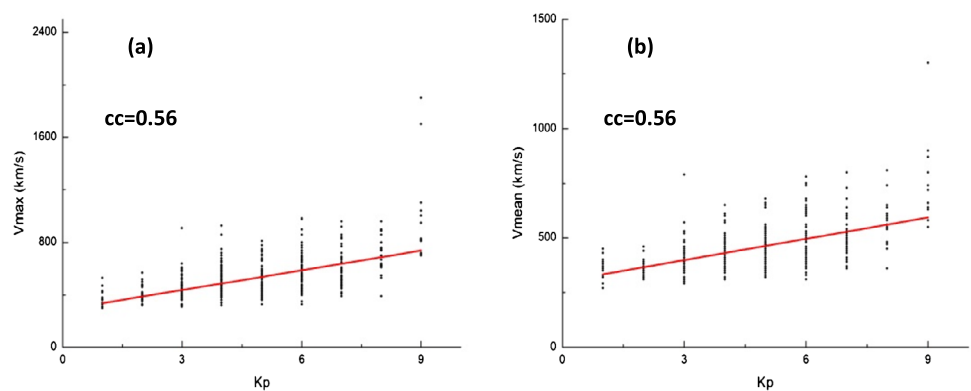
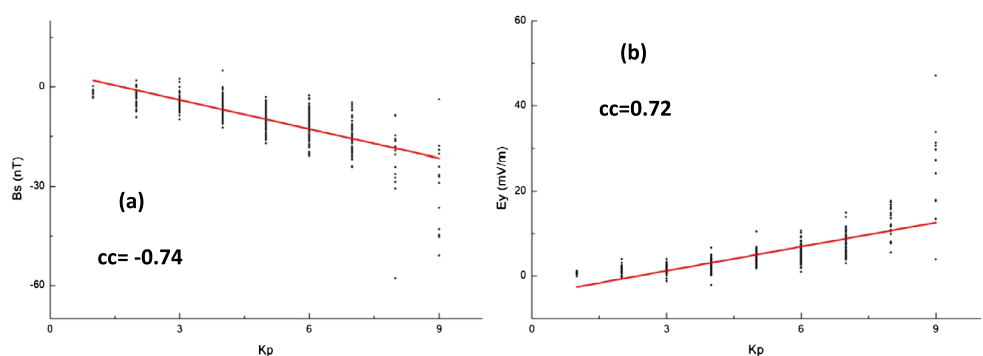


Fig. 5 A correlation diagram of the minimum value of the IMF south component B_s (left panel) and of the maximum value of the dawn-to-dusk E_y convective field (right panel) versus the Kp index values is presented



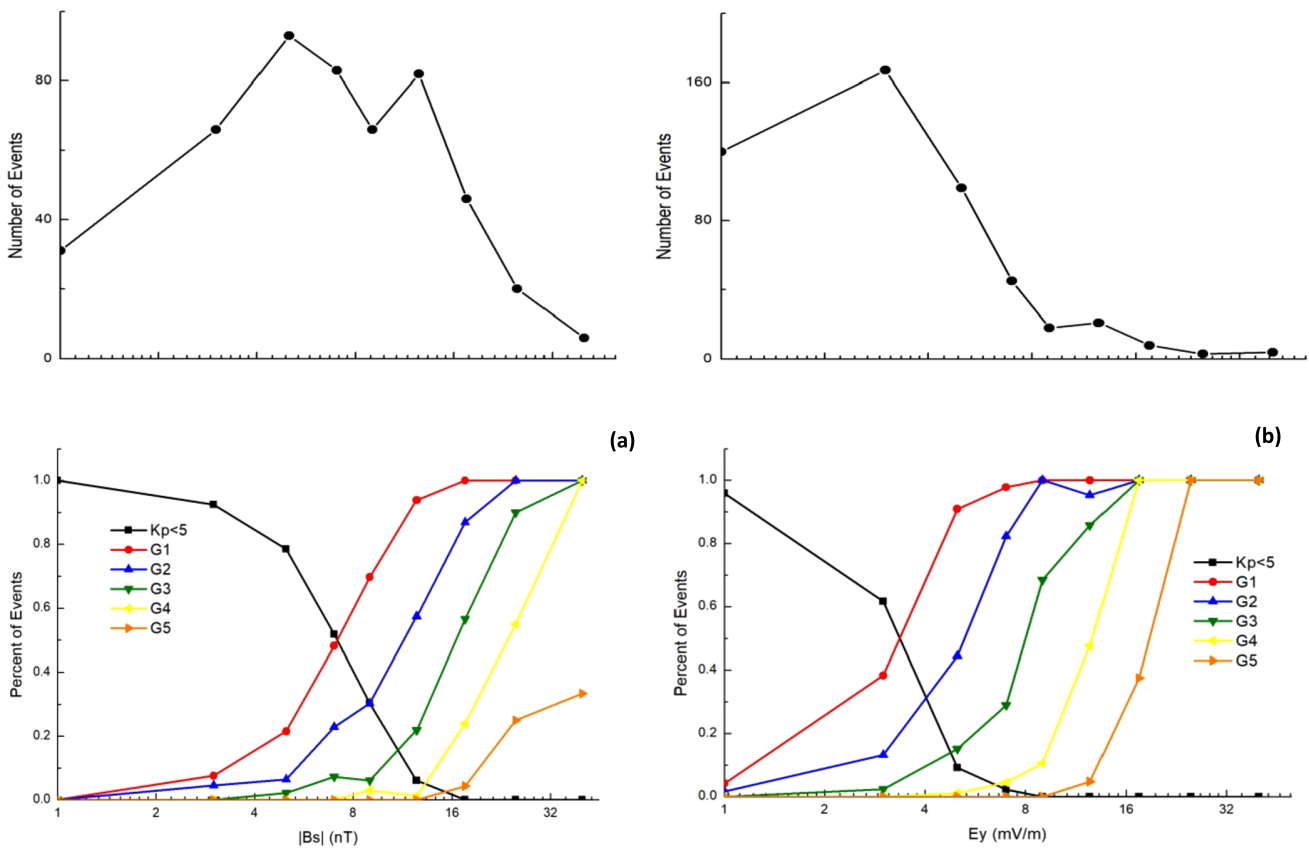


Fig. 6 The variation of the probability of generated storms (or percent of events) that reach at a specific storm class (based on NOAA “G” scale) versus the minimum absolute B_s value of the interplanetary magnetic field (left lower panel) and the maximum E_y value of the con-

vective electric field of each ICME at L1 point (right lower panel). In the upper panels the number of the ICME events in each range of $|B_s|$ (left upper panel) and E_y (right upper panel) values is given during the years 1996–2017

son and Cane 2011 and references therein). Our results are in consistent with the results of the study of Richardson and Cane (2011), where the cc was 0.78 and 0.88 respectively, for solar cycle 23 (1995–2009). These slight differences can be explained by two factors. We used in our study the integer and not the decimal values of K_p index, which may influences the accuracy of the cc , and also our data are for two solar cycles (1996–2017), which seem to differ in their intensity (Figs. 1 and 2).

The probability of an ICME generating a specific class of GS or not, depending on its minimum $|B_s|$ value (left lower panel) and maximum E_y value (right lower panel) are given in Fig. 6. We can see that for example, an ICME with a value of approximately $|B_s| \approx 12.5$ nT (value between 10 and 15 nT), has a $\sim 5\%$ probability of not generating a GS ($K_p < 5$), a $\sim 95\%$ probability of generating a G1 storm ($K_p = 5$), a $\sim 55\%$ probability of generating a G2 storm ($K_p = 6$), a $\sim 20\%$ probability for G3 storm ($K_p = 7$), and no chance of generating a G4 or G5 storms ($K_p = 8$ and 9). Moreover, if we have for example the value $E_y \sim 7$ mV/m (e.g. with value between 6 and 8 mV/m), there is $\sim 2\%$ probability of not generating a GS ($K_p < 5$),

$\sim 98\%$ for generating a G1 storm, $\sim 82\%$ for generating a G2 storm, $\sim 30\%$ for generating a G3 storm, $\sim 4\%$ for generating a G4 storm and finally no chance for G5 storm. The results are inconsistent with the ones of Richardson and Cane (2011). The points for 50% probability of generating GSs are found at the values: $|B_s| \sim 7$ nT and $E_y \sim 3$ mV/m for G1 storms, $|B_s| \sim 10$ nT and $E_y \sim 5$ mV/m for G2 storms, $|B_s| \sim 15$ nT and $E_y \sim 8$ mV/m for G3 storms, and $|B_s| \sim 22$ nT and $E_y \sim 12.5$ mV/m for G4 storms. For G5 we have only 11 events, insufficient for the probabilities to be measured in a useful level, but it seems that they are approximately at $|B_s| \sim 35\text{--}40$ nT and $E_y \sim 20$ mV/m. In the upper panels of this Figure the number of the ICME events in each range of $|B_s|$ (left upper panel) and E_y (right upper panel) values is given during the years 1996–2017. The black line at the lower panels of Fig. 6 ($K_p < 5$ means there was no GS generated from the passing ICME) is the probability of an ICME to generate a disturbance with $K_p < 5$ which means that this lines drops as the values of B_s and E_y increase in the ICME because these values are very important for the generation of a geomagnetic disturbance due to their role at the reconnection process in the dayside of the

Earth’s magnetosphere. The colored lines are the probabilities for generation of specific scales of GSs, as explained in the panel.

3.3 ICMEs and Dst index

Moreover the geoeffectiveness of the ICMEs according to Dst index (Zhang et al. 2007; Richardson and Cane 2011) was also considered. The used Dst index data from the WDC for Geomagnetism, Kyoto are the final values up to 2014, the provisional values for 2015–2016 and the quicklook values thereafter. Some (a few) provisional and quicklook values may be revised in the future, with changes only a few nT, which means that our results will not be efficiently changed. It is noted from Fig. 7 that 50.9% (252 out of 495 events) of the ICMEs didn’t generate a GS, while 49.1% (243 events) generated a GS. We also notice that 29.5% (146 out of 495) of the events (ICMEs and their possible sheath region and Shock) generated a Moderate storm, 15.3% (76 out of 495) generated a strong storm ($-50 < \text{Dst} \leq -100$ nT), 3% (16 events) generated a severe storm and 1% (5 events) generated a great storm. This means that only a quarter of the

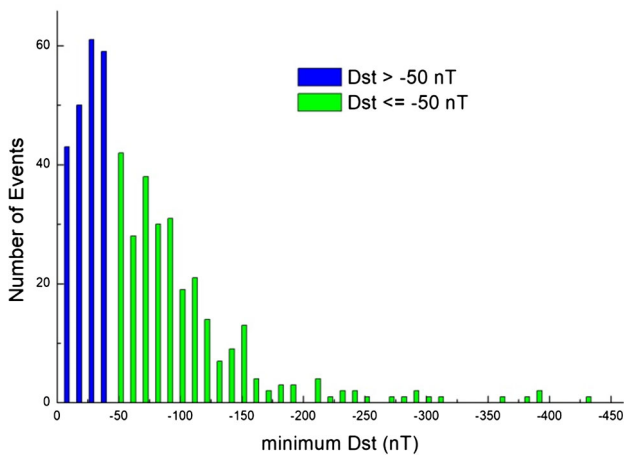
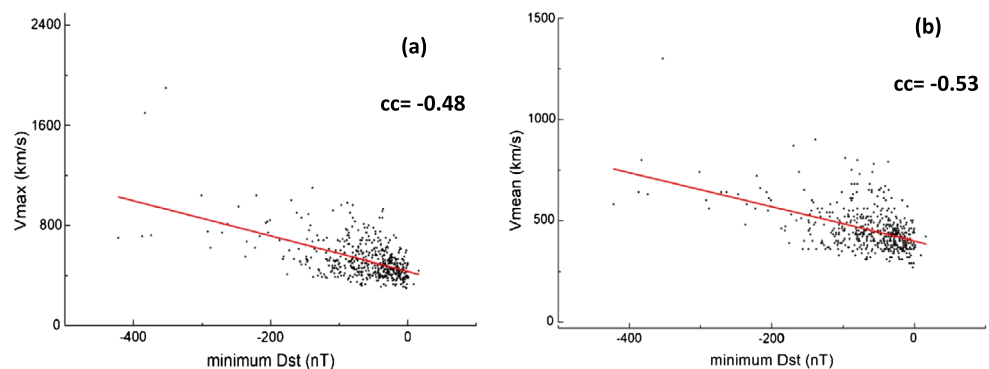


Fig. 7 Distribution of the number of the geomagnetic storms-associated with ICMEs ($\text{Dst} \leq -50$ nT, blue color) and those non-storm events ($\text{Dst} > -50$ nT, green color) under the affection of the ICMEs during the years 1996–2017

Fig. 8 Correlation diagram of the ICME V_{max} (left panel) and of the ICME V_{mean} (right panel) velocity with the minimum Dst values



ICMEs of the last two solar cycles 23 and 24 are associated with intense storms ($\text{Dst} \leq -100$ nT) (Tsurutani and Gonzalez 1997; Richardson and Cane 2011), even though the ICMEs are considered as important drivers of the intense GSs.

A correlation diagram of the mean ICME (solar wind) velocity (left panel) and the maximum velocity of the event (ICME/Sheath and the possible shock) (right panel) with the minimum Dst value of each event is presented in Fig. 8. It’s clear again (as well as with Kp) that the correlation of the minimum Dst value with these velocities is moderate (cc is -0.48 and -0.53 accordingly). Thus, the velocities of an ICME structure are good but not solid space weather forecasting factors. So we must turn our view on the other important space weather factors, the south component B_s of the ICME’s magnetic flux structure and the y-component of the convective electric field E_y of solar wind at L1 point, measured by WIND and ACE spacecrafts. Figure 9 (left and right panels) shows that the correlation of minimum Dst is much higher with these factors (cc is 0.88 and -0.87 accordingly), confirming previous studies that showed that B_s and E_y play a vital role on space weather effects due to the magnetic reconnection process between the solar wind magnetic field and the magnetosphere (Tsurutani and Gonzalez 1997; Ji et al. 2010; Richardson and Cane 2010; Paouris and Mavromichalaki 2017a, 2017b).

We now consider the probability of an ICME generating GS, depending on the Dst index. Figure 10 (left and right panels) demonstrates that probabilities (or the percent of events that occurred during the solar cycles 23 and 24) of generating specific scales of GSs, depending on the minimum $|B_s|$ and maximum E_y values of the events. We see that for an ICME with the value of, for example, $|B_s| \approx 12.5$ nT (e.g. values between 10 and 15 nT) there is a 10% probability of not generating a GS, 90% probability of generating a Moderate GS, 34% probability of generating a Strong GS and 0% for intense storms (see Table 1 for scales). We also notice that when $|B_s|$ is at least 17.5 nT (e.g. 15–20 nT and above) we have 0% chance of not generating GS, which means that ICMEs with value $|B_s| > 15$ nT will surely gen-

Fig. 9 Correlation diagram of the minimum value of the south component B_s of the interplanetary magnetic field (left panel) and the maximum value of the y -component E_y of the convective electric field (right panel) versus the minimum Dst index values

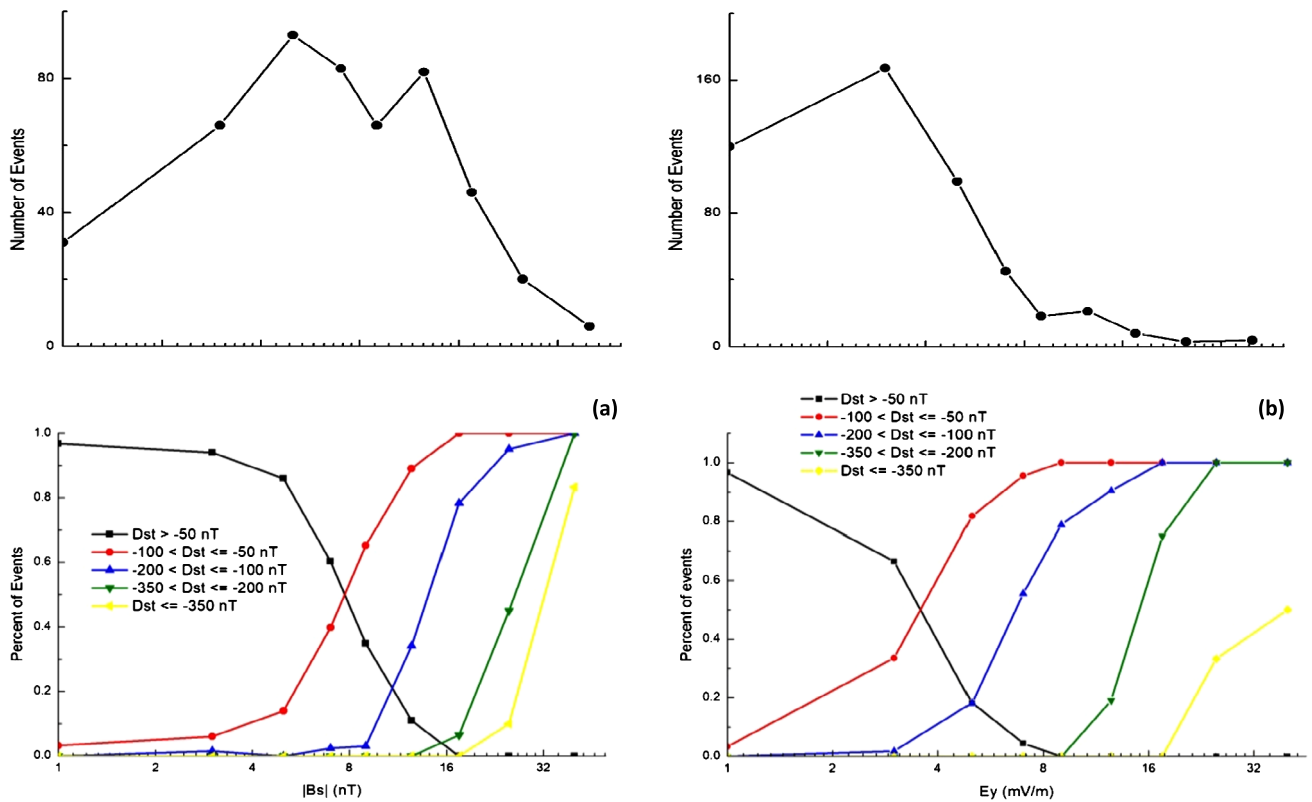
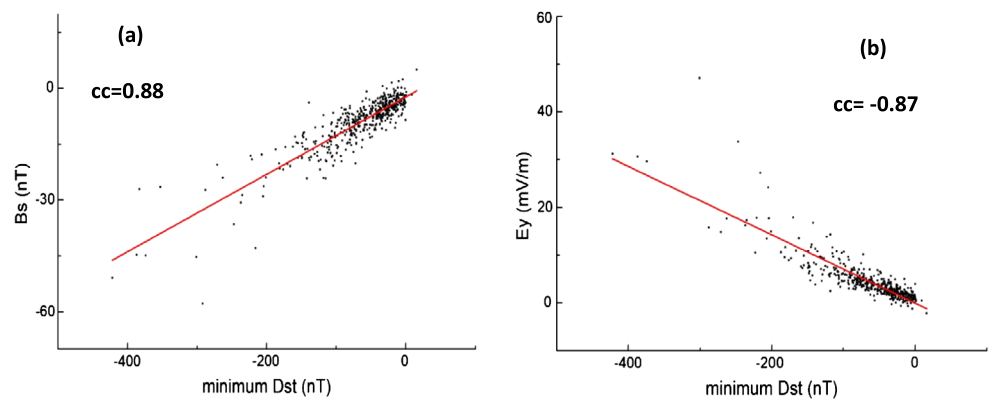


Fig. 10 Minimum absolute B_s value of the interplanetary magnetic field (left panel) and maximum E_y value of the convective electric field of each ICME at L1 point (right panel) versus the variation of probabilities (or percent of events) for generation of specific storm scale based

on Dst index scale, during the years 1996–2017. On the upper panels the number of ICME events in each range of $|B_s|$ (left) and E_y (right) values are given

erate a GS. For E_y , this value seems to be at 8–10 mV/m and above. The points for 50% probability of generating specific GSs scales are found at: $|B_s| \approx 8$ nT and $E_y \approx 4$ mV/m for Moderate storms, $|B_s| \approx 13$ nT and $E_y \approx 6$ mV/m for Strong storms, $|B_s| \approx 26$ nT and $E_y \approx 16$ mV/m for Severe storms. For Great storms we have very few events to give accurate probabilities, although here we find them at the values $|B_s| \approx 32$ nT and $E_y \approx 36$ mV/m. The results are also consistent with those ones of Richardson and Cane (2011) for the solar cycle 23.

3.4 ICMEs and their velocities

The fact that there are no in-situ observations of the reliable geoeffective factors B_s and E_y makes the ICMEs geoeffectiveness forecasting more complicated. We can only use upstream monitors at L1 point (such as WIND and ACE), which provides us with little warning time of upcoming events (less than an hour) (Richardson and Cane 2011). However, the velocities (mean and maximum) of the ICME structures (ejecta, sheath and possible shock) seem to have

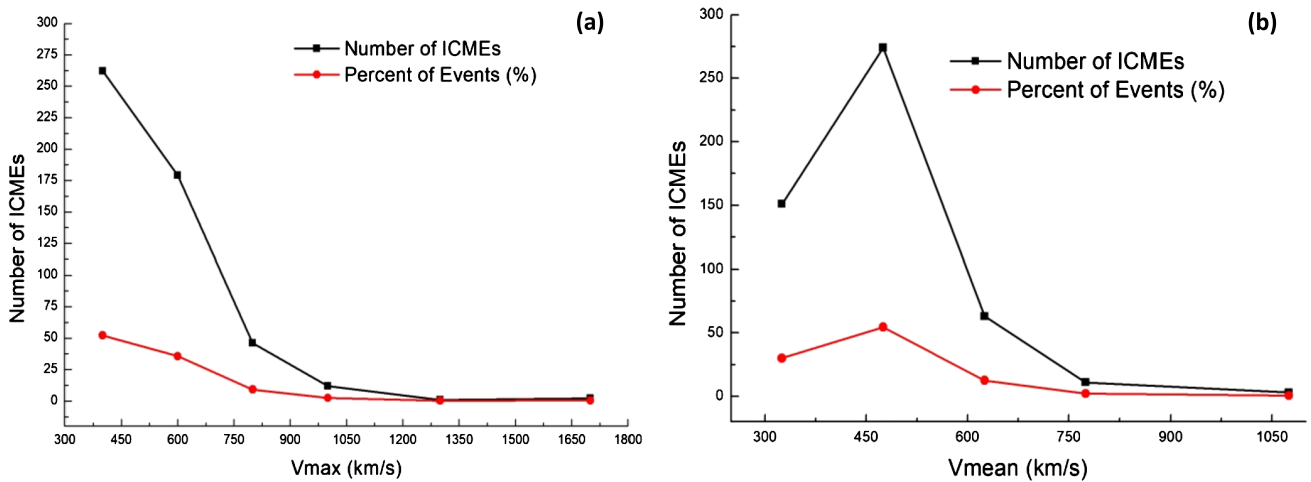


Fig. 11 The number (black color) and percentages (red color) of ICMEs versus the ICMEs Vmax (left panel) and the ICMEs Vmean (right panel) velocities during 1996–2017) are given

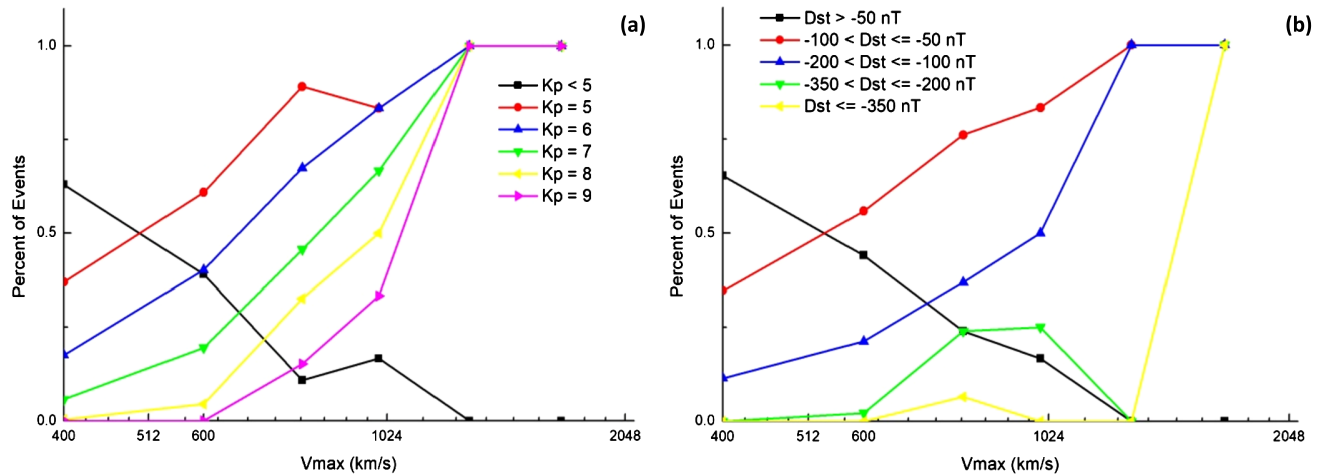


Fig. 12 The variation of probabilities (or percent of events) for generation of a specific storm scale according to Kp (left panel) and to Dst indices values (right panel) versus the maximum (Vmax) values

of velocity of the ICMEs recorded during the solar cycles 23 and 24 (1996–2017) is illustrated

less potential to geoeffectiveness forecasting, but they can be estimated remotely around 1 to 4 days in advance. We can use these data to make estimations on the probability of an ICME generating specific Geomagnetic Storm level. In Fig. 11 (a and b) we see the maximum and mean velocities distributions over the solar cycles 23 and 24. The most probable value for the maximum velocity is 460 km/s and 370 km/s for the mean velocity. In Fig. 12 we can see the probabilities of generating specific GS scales depending on the maximum velocity of the ICMEs. Two results can be outlined. The first is that the maximum velocity of the ICMEs can be more geoeffective according to Kp index (i.e. affect more easily the Kp index than Dst). This can be ascertained by the higher storm-generation probabilities from lower velocities of the ICMEs according to Kp index. The second

is that the probabilities for Severe and Great storms for Kp are also higher. This is due to more events for Kp = 8 and Kp = 9 (33 events in total) than Dst ≤ -200 nT (12 events), which can also be explained by the different magnetospheric current systems that affect these indices (Ganushkina et al. 2018 and references therein). The estimations for Severe and Great storms, according to Dst, are not very good due to low number of events and hence cannot be used efficiently for space weather forecasting purposes. This confirms our previous results for the correlation of ICMEs mean and maximum velocities versus the geomagnetic activity (Kp and Dst index, see Sects. 3.2 and 3.3). It is noted that only for low and medium velocities of the ICMEs, we can have good estimations of the probabilities of generating specific storm scales, due to large number of events.

4 Conclusions and discussion

In this work the relation of 502 ICMEs (although excluding 7 due to lack of data) with the Geomagnetic Storms (GSs), during the last two solar cycles 23 and 24 were investigated. At first, the number of the ICME events was compared with the annual number of GSs during these two solar cycles. The most geoeffective parameters of the ICMEs and the way they affect the magnetosphere, depending on their impact on Kp and Dst geomagnetic indices were analyzed. We also considered the mean and maximum velocities of the ICMEs according to Catalogue of Richardson and Cane (2019) for both solar cycles. Summarizing our results are the following:

- (a) Despite the fact that ICMEs are characterized as important drivers of the geomagnetic storms (GSs), we found out that only $\sim 50\%$ of the ICMEs were generated GSs during the years 1996–2017. Moreover, $\sim 23\%$ of them were generated intense GSs (with $Dst \leq -100$ nT and/or $Kp \geq 7$) and the probability for severe storms was 7% with $Kp \geq 8$ and 4% with $Dst \leq -200$ nT. Similar results were found also by Richardson and Cane (2011) for the time period 1995–2009. We note that in this study the duration of the events (i.e. the duration of the southward component Bs of the events) were not considered, although it seems to have an important role on their geoeffectiveness (O'Brien and McPherron 2000; Ji et al. 2010).
- (b) The southward component of the interplanetary magnetic field Bs and the dawn-to-dusk (y-component) convective electric field Ey, measured at L1 point by ACE spacecraft obtained from OMNIWeb presents a much better correlation with the geoeffectiveness, as it was expected due to their role in the magnetic reconnection process in the dayside of the magnetosphere (Tsurutani and Gonzalez 1997). Due to the lack of distant in-situ observations, we cannot use them to make space weather forecasting enough time before the ICME encounters the magnetosphere, unless there is a good method to measure or forecast these factors several hours/days before the disturbance arrives. There have been many promising steps to this direction (e.g. Riley et al. 2017; Riley and Love 2017) for predicting the Bs component of the IMF. With such techniques, and along with the results of this study, space weather forecasters will have a very good and reliable tool for forecasting the future geospace activity enough time in advance to take all the necessary measures and precautions. We also notice that the correlations of these factors (Bs and Ey) are slightly better with the minimum Dst ($cc = 0.88$ and -0.87) compared to the Kp index ($cc = -0.74$ and 0.72) respectively (Table 3). This difference can possibly be explained by the fact that these two indices are affected

Table 3 The correlation coefficient of the GSs measured with Kp and Dst index versus the plasma parameters Bs and Ey of the ICMEs, for the years 1996–2017

	Southward Bs (nT)	Ey (mV/m)
Storms according to Kp	-0.74	0.72
Storms according to Dst	0.88	-0.87

Table 4 The correlation coefficient of the GSs measured with Kp and Dst index versus the plasma parameters Bs and Ey of the ICMEs, for the years 1996–2017

	Mean ICME velocity	Max ICME velocity
Storms according to Kp	0.56	0.56
Storms according to Dst	-0.53	0.48

by different magnetospheric currents (Ganushkina et al. 2018 and references therein). More specifically, the Kp index can also be affected by the substorm mechanism through the magnetotail current and field-aligned currents which means that with Kp we count more events. This can also explain the difference in GSs numbers in Fig. 1b and 1c recorded by these two indices. The results seem to be in accordance with the results of the work by Richardson and Cane (2011) for the solar cycle 23.

- (c) The mean and maximum velocities of the ICMEs have a moderate correlation with the GSs, both with Kp and Dst indices (Table 4), thus they are considered as moderate space weather forecasting factors. However, velocities of the ICMEs can be measured from long distance by coronagraphs on spacecrafts (e.g. from LASCO/SOHO or STEREO coronagraphs) or by all-sky imagers (e.g. Solar Mass Ejection Imager) (Richardson and Cane 2011 and references therein), making them important factors for geoeffectiveness's prediction of ICMEs for the time being, due to lack of in-situ observations of other important geoeffective plasma parameters of the ICMEs. Thus, we can have probabilities of generation of specific GSs scales using these velocities of ICME-structures.
- (d) To compare our results with the similar study of Richardson and Cane (2011) for the geoeffectiveness of the ICMEs and their probabilities of generating specific GS scales, we summarized our results in the following Tables 5, 6 and 7.

In Tables 5 and 6 we see the values of the parameters Bs and Ey that an ICME must have in order to have 50% probability to generate specific Geomagnetic Storm scale, according to Kp and Dst indices. For example, in order for an ICME to have 50% probability to generate a G3 storm ($Kp = 7$), its Bs value must be at

Table 5 The minimum values of parameters Bs and Ey of the ICMEs that are required in order to have 50% probability of generating specific geomagnetic storm scales by the ICMEs. The storms are referred according to Kp index. The values are for cycle 23 (from the study of Richardson and Cane 2011) and for cycles 23 and 24 (from this study)

Geomagnetic storms with probability >50% – Kp index		
Plasma parameters versus indices	Cycle 23 Richardson and Cane (2011)	Cycles 23 and 24 This work
Bs – G1	–	7 nT
Bs – G2	–	10 nT
Bs – G3	–	15 nT
Bs – G4	–	22 nT
Bs – G5	–	35–40 nT mV/m
Ey – G1	3.5 mV/m	3 mV/m
Ey – G2	4.5 mV/m	5 mV/m
Ey – G3	8 mV/m	8 mV/m
Ey – G4	12 mV/m	12.5 mV/m
Ey – G5	30–40 mV/m	20 mV/m

Table 6 The minimum values of parameters Bs and Ey of the ICMEs that are required in order to have 50% probability of generating specific geomagnetic storm scales by the ICMEs. The storms are referred according to Kp index. The values are for cycle 23 (from the study of Richardson and Cane 2011) and for cycles 23 and 24 (from this study)

Geomagnetic storms with probability >50% – Dst index		
Plasma parameters versus indices	Cycle 23 Richardson and Cane (2011)	Cycles 23 and 24 This work
Bs – Moderate GS	8 nT	8 nT
Bs – Strong GS	12 nT	13 nT
Bs – Severe GS	20 nT	26 nT
Bs – Great GS	~ 28 nT	32 nT
Ey – Moderate GS	3 mV/m	4 mV/m
Ey – Strong GS	6 mV/m	6 mV/m
Ey – Severe GS	15 mV/m	16 mV/m
Ey – Great GS	~30 mV/m	36 mV/m

least 15 nT and the Ey must be at least 8 mV/m. For a 50% probability of a Strong storm ($Dst \leq -100$ nT) the ICME must have a Bs at least 12 nT and an Ey at least 6 mV/m, according to these two studies.

In Table 7 we see the correlation coefficients for every association of the values of the first column. Again we see similar values, which means that the geoeffectiveness of the values Bs, Ey and the velocities of the ICMEs is not affected much by the solar cycles. We only notice a difference at the value of Ey, according to Kp only. This difference can again be explained by the fact that Kp index can be affected by the geomagnetic sub-storm system, hence provide us with events that are not

Table 7 Correlation coefficients of the different parameters used in this work in relation to the Kp index (upper) and to the Dst index (lower) during solar cycle 23 (Richardson and Cane 2011) and during the cycles 23 and 24 obtained from this work

Correlation coefficients		
Plasma parameters versus indices	Cycle 23 Richardson and Cane (2011)	Cycles 23 and 24 This work
<i>For Kp index</i>		
Vmax–Kp	0.58	0.56
Vmean–Kp	–	0.56
Bs–Kp	0.78	–0.74
Ey–Kp	0.87	0.72
<i>For Dst index</i>		
Vmax–Dst	–0.54	–0.48
Vmean–Dst	–	–0.53
Bs–Dst	0.89	–0.88
Ey–Dst	–0.87	–0.87

considered as GSs by the Dst index (with low intensity of course). We also notice that the correlation coefficients of our study compared to the ones of the study of Richardson and Cane (2011) have different sign due to the fact that we maintained in this work the negative values of Bs, while in Richardson and Cane (2011) the values were turned positive. This point does not affect the general results.

Even though this study was for both cycles 23 and 24, we see only small differences in values of the geoeffectiveness of the ICMEs between this study and the study of Richardson and Cane (2011) for solar cycle 23. We notice that on the Tables 5 and 7 some points are missing, because they are not provided in the other study. The fact that the plasma parameters and the correlation coefficients are similar in values means that, in general, the role of each parameter to the geoeffectiveness of the ICMEs does not change per solar cycle.

(e) Despite the moderate correlation between the mean and maximum velocities of ICME-structures and their geoeffectiveness, we see an increase of GSs occurrence together with an increase of mid and high-velocity ICMEs during rising and around maximum phases, especially at solar cycle 23 (see Figs. 1b, c, d and 2). It is also clear that during the first stages of the declining phases of solar cycles, we have an increase both in number of GSs and in the velocity of the ICMEs together with a decrease of the number of the ICMEs, which means that the faster and more geoeffective ICMEs alone cannot justify the big increase of the number of GSs during that period. Hence, different source drivers of strong geomagnetic activity increase in numbers. Such drivers

are high speed solar wind streams from Coronal Holes (Gonzalez et al. 1999, 2011; Gerontidou et al. 2018).

- (f) According to both the number of GSs and the numbers and characteristic velocities of ICMEs, we see that the two solar cycles have big differences in intensity. More specifically, solar cycle 23 seems to be stronger in all factors, something that has been observed in other studies too (e.g. Chi et al. 2016). For example, the mean and maximum velocities are higher in every phase of cycle 23 than 24, but the two cycles seem to have the same trend, concerning the occurrence of GSs and numbers and velocities of ICMEs. Also, they both have faster ICMEs during the declining phases than the rising and maximum phases (Figs. 1b, c, and 2a, b). The maximum annual numbers of the GSs and the ICMEs seem to be in accordance with the SSN maximum for both cycles, with ~ 1 year difference. However, for the cycle 23 we see a dramatic increase of geomagnetic activity at 2003, which is not followed by an increase in the number of ICMEs. Although this year may be an exception and not a rule for the solar cycles, during the declining phase of solar cycles there is a decrease (except the years 2005 and 2015) in numbers and geoeffectiveness of the ICMEs (Fig. 1d) which is not exactly followed by the same decrease in geomagnetic activity. This confirms the previous results about the increase in numbers of other geoeffective solar sources of the GSs.

In conclusion, we infer that ICME velocities can be used, for now, for space weather forecasting due to the fact that they can be measured distantly and therefore we can have sufficient warning time for their possible geoeffectiveness, depending on their velocity measures (statistically). There are also models that can estimate very well the arrival time of an ICME and its possible Shock at the Earth's magnetosphere (e.g. the EAMv2 model, see: Paouris and Mavromichalaki 2017a, 2017b). Such tools, together with the distant measurements of the velocities, can be used at space weather forecasting, as it is already happening, for example, at Athens Space Weather Forecasting Center (cosray.phys.uoa.gr/index.php/space-weather-report). The results for the probabilities of generating specific storm scales from this work, using the velocities, can be useful to such forecasting methods.

However these methods cannot yet be used for the more geoeffective parameters Bs and Ey of the ICMEs, although numerical and empirical models for forecasting the orientation and magnitude of the magnetic field of the ICMEs (and the solar wind in general) may provide a useful and reliable tool for space weather forecasting, using also its correlation with the geoeffectiveness given in this work. Moreover, we note that during 2018, eight ICMEs were recorded in the catalogue, but only one of them gave rise to a geomagnetic storm, at 25/08/2018 with minimum Dst = -174 nT

(Richardson and Cane's ICMEs catalogue). Thus, not including these eight events should not affect the main results of this work. Also, 7 of the ICMEs during 1996–2017 showed errors in the data of Bs and Ey according to data from OMNIWeb, so we didn't include them in our analysis.

Acknowledgements The authors appreciate the OMNI Database and the WDC, Kyoto Database for their contribution in data for this work. The OMNI data (Kp and plasma data) were obtained from GSFC/SPDF OMNIWeb and the Dst data were obtained from the WDC for Geomagnetism. We also acknowledge SILSO Database for its contribution with SSN data. Finally, the authors are grateful to I.G. Richardson and H.V. Cane for their contribution in the ICMEs data with their comprehensive catalogue and studies.

Conflict of Interest The authors indicate that there is no conflict of interest.

Publisher's Note Springer Nature remains neutral with regard to jurisdictional claims in published maps and institutional affiliations.

References

- Borovsky, E.J., Shprits, Y.: Is the Dst index sufficient to define all geospace storms? *J. Geophys. Res.* **122**, 11543 (2017). <https://doi.org/10.1002/2017JA024679>
- Chi, Y., Shen, S., Wang, Y., Xu, M., Ye, P., Wang, S.: Statistical study of the interplanetary coronal mass ejections from 1995 to 2015. *Sol. Phys.* **291**, 2419 (2016). <https://doi.org/10.1007/s11207-016-0971-5>
- Daglis, I.A., Kozyra, J.U., Kamide, Y., Vassiliadis, D., Sharma, A.S., Liemohn, M.W., Gonzalez, W.D., Tsurutani, B.T., Lu, G.: Intense space storms: critical issues and open disputes. *J. Geophys. Res.* **108**, 1208 (2003). <https://doi.org/10.1029/2002JA009722>
- Dungey, J.R.: Interplanetary magnetic field and auroral zones. *Phys. Rev. Lett.* **6**, 47 (1961). <https://doi.org/10.1103/PhysRevLett.6.47>
- Echer, E., Gonzalez, W.D., Tsurutani, B.T., Gonzalez, A.L.C.: Interplanetary conditions causing intense geomagnetic storms ($Dst \leq -100$ nT) during solar cycle 23 (1996–2006). *J. Geophys. Res.* **113**, A05221 (2008). <https://doi.org/10.1029/2007JA012744>
- Echer, E., Korth, A., Bolzan, M.J.A., Friedel, R.H.W.: Global geomagnetic responses to the IMF B_z fluctuations during the September/October 2003 high speed stream intervals. *Ann. Geophys.* **35**, 853 (2017). <https://doi.org/10.5194/angeo-35-853-2017>
- Feynman, J., Gabriel, S.B.: On space weather consequences and predictions. *J. Geophys. Res.* **105**, 10543 (2000). <https://doi.org/10.1029/1999JA000141>
- Galata, E., Ioannidou, S., Papailiou, M., Mavromichalaki, H., Paravolidakis, K., Kouremeti, M., Rentifis, L., Simantirakis, E., Trachanas, K.: *Astrophys. Space Sci.* **138**, 362 (2017). <https://doi.org/10.1007/s10509-017-3118-8>
- Ganushkina, N.Yu., Liemohn, M.W., Dubyagin, S.: Current systems in the Earth's magnetosphere. *Rev. Geophys.* **56**, 309 (2018). <https://doi.org/10.1002/2017RG000590>
- Gerontidou, M., Mavromichalaki, H., Daglis, T.: High-speed solar wind streams and geomagnetic storms during solar cycle 24. *Sol. Phys.* **131**, 293 (2018). <https://doi.org/10.1007/s11207-018-1348-8>
- Gonzalez, W.D., Joselyn, J.A., Kamide, Y., Kroehl, H.W., Rostoker, G., Tsurutani, B.T., Vasyliunas, V.M.: What is a geomagnetic storm? *J. Geophys. Res.* **99**, 5771 (1994). <https://doi.org/10.1029/93JA02867>

- Gonzalez, W.D., Tsurutani, B.T., Gonzalez, A.L.: Interplanetary origin of geomagnetic storms. *Space Sci. Rev.* **88**, 529 (1999). <https://doi.org/10.1023/A:1005160129098>
- Gonzalez, W.D., Echer, E., Tsurutani, B.T., Gonzalez, A.L.: Interplanetary origin of intense, superintense and extreme geomagnetic storms. *Space Sci. Rev.* **158**, 69 (2011). <https://doi.org/10.1007/s11214-010-9715-2>
- Gopalswamy, N., Akiyama, S., Yashiro, S., Xie, H., Mäkelä, P., Michalek, G.: Anomalous expansion of coronal mass ejections during solar cycle 24 and its space weather implications. *Geophys. Res. Lett.* **41**, 2673 (2014). <https://doi.org/10.1002/2014GL059858>
- Gosling, J.T., McComas, D.J., Philips, J.L., Bame, S.J.: Geomagnetic activity associated with Earth passage of interplanetary shock disturbances and coronal mass ejections. *J. Geophys. Res.* **96**, 7831 (1991). <https://doi.org/10.1029/91JA00316>
- Huttunen, K.E.J., Schwenn, R., Bothmer, V., Koskinen, H.E.: Properties and geoeffectiveness of magnetic clouds in the rising, maximum and early declining phases of solar cycle 23. *Ann. Geophys.* **23**, 625 (2005). <https://doi.org/10.5194/angeo-23-625-2005>
- Ji, E.-Y., Moon, Y.-J., Kim, K.-H., Lee, D.-H.: Statistical comparison of interplanetary conditions causing intense geomagnetic storms ($\text{Dst} \leq -100$ nT). *J. Geophys. Res.* **115**, A10232 (2010). <https://doi.org/10.1029/2009JA015112>
- Lakhina, G.S., Tsurutani, B.T.: Geomagnetic storms: historical perspective to modern view. *Geosci. Lett.* **3**, 5 (2016). <https://doi.org/10.1186/s40562-016-0037-4>
- Loewe, C.A., Prölss, G.W.: Classification and mean behavior of magnetic storms. *J. Geophys. Res.* **102**, 14209 (1997). <https://doi.org/10.1029/96JA04020>
- Mavromichalaki, H., Vassilaki, A.: Fast plasma streams recorded near the Earth during 1985–1996. *Sol. Phys.* **183**, 181 (1998). <https://doi.org/10.1023/A:1005004328071>
- Mayaud, P.N.: Derivation, meaning and use of geomagnetic indices. In: *Geophys. Monogr. Ser.*, vol. 22. AGU, Washington (1980)
- Menvielle, M., Berthelier, A.: The K -derived planetary indices: description and availability. *Rev. Geophys.* **29**, 415 (1991). <https://doi.org/10.1029/91RG00994>
- Mustajab, F., Badruddin: Geoeffectiveness of the interplanetary manifestations of coronal mass ejections and solar-wind stream-stream interactions. *Astrophys. Space Sci.* **331**, 91 (2011). <https://doi.org/10.1007/s10509-010-0428-5>
- O'Brien, T.P., McPherron, R.L.: An empirical space analysis of ring current dynamics: solar wind control of injection and decay. *J. Geophys. Res.* **105**, 7707 (2000). <https://doi.org/10.1029/1998JA000437>
- Owens, M.J., Cargill, P.J., Pagel, C., Siscoe, G.L., Crooker, N.U.: Characteristic magnetic field and speed properties of interplanetary coronal mass ejections and their sheath regions. *J. Geophys. Res.* **110**, A01105 (2005). <https://doi.org/10.1029/2004JA010814>
- Paouris, E., Mavromichalaki, H.: Interplanetary coronal mass ejections resulting from Earth-directed CMEs using SOHO and ACE combined data during solar cycle 23. *Sol. Phys.* **292**, 24 (2017a). <https://doi.org/10.1007/s11207-017-1050-2>
- Paouris, E., Mavromichalaki, H.: Effective acceleration model for the arrival time of interplanetary shocks driven by coronal mass ejections. *Sol. Phys.* **292**, 11 (2017b). <https://doi.org/10.1007/s11207-017-1212-2>
- Rama, R.P.V.S., Gopi, K.S., Vara, P.J., Prasad, S.N.V.S., Prasad, D.S.V.V.D., Niranjana, K.: Geomagnetic storms effects on GPS based navigation. *Ann. Geophys.* **27**, 2101 (2009). <https://doi.org/10.5194/angeo-27-2101-2009>
- Richardson, I.G., Cane, H.V.: Near-Earth interplanetary coronal mass ejections during solar cycle 23 (1996–2009): catalogue and summary of properties. *Sol. Phys.* **264**, 189 (2010). <https://doi.org/10.1007/s11207-010-9568-6>
- Richardson, I.G., Cane, H.V.: Geoeffectiveness (Dst and Kp) of interplanetary coronal mass ejections during 1995–2009 and implications for storm forecasting. *Space Weather* **9**, S07005 (2011). <https://doi.org/10.1029/2011SW000670>
- Richardson, I.G., Cliver, E.W., Cane, H.V.: Sources of geomagnetic storms for solar minimum and maximum conditions during 1972–2000. *Geophys. Res. Lett.* **28**, 2569 (2001). <https://doi.org/10.1029/2001GL013052>
- Riley, P., Love, J.J.: Extreme geomagnetic storms: probabilistic forecasts and their uncertainties. *Space Weather* **15**, 53–64 (2017). <https://doi.org/10.1002/2016SW001470>
- Riley, P., Ben-Num, M., Linker, J.A.: Forecasting the properties of the solar wind using simple pattern recognition. *Space Weather* **15**, 526–540 (2017). <https://doi.org/10.1002/2016SW001589>
- Thomson, A.W.P., McKay, A.J., Clarke, E., Reay, S.J.: Surface electric fields and geomagnetically induced currents in the Scottish Power grid during the 30 October 2003 geomagnetic storm. *Space Weather* **3**, S11002 (2005). <https://doi.org/10.1029/2005SW000156>
- Tsurutani, B.T., Gonzalez, W.D.: The interplanetary causes of magnetic storms: a review. In: *Magnetic Storms*. *Geophys. Monogr. Ser.*, vol. 98, p. 77 (1997). <https://doi.org/10.1029/GM098p0077>
- Tsurutani, B.T., Gonzalez, W.D., Tang, F., Akasofu, S.I., Smith, E.J.: Origin of interplanetary southward magnetic fields responsible for major magnetic storms near solar maximum (1978–1979). *J. Geophys. Res.* **93**, 8519 (1988). <https://doi.org/10.1029/JA093iA08p08519>
- Welling, D.T.: The long-term effects of space weather on satellite operations. *Ann. Geophys.* **28**, 1361 (2010). <https://doi.org/10.5194/angeo-28-1361-2010>
- Zhang, G., Burlaga, L.F.: Magnetic clouds, geomagnetic disturbances, and cosmic ray decreases. *J. Geophys. Res.* **93**, 2511 (1988). <https://doi.org/10.1029/JA093iA04p02511>
- Zhang, J., Richardson, I.G., Webb, D.F., Gopalswamy, N., Huttunen, E., Kasper, J.C., Nitta, N.V., Poomvises, W., Thompson, B.J., Wu, C.-C., Yashiro, S., Zhukov, A.N.: Solar and interplanetary sources of major geomagnetic storms ($\text{Dst} \leq -100$ nT) in 1996–2005. *J. Geophys. Res.* **112**, A10102 (2007). <https://doi.org/10.1029/2007JA012321>